

Selected papers presented at the XIII All-Polish Seminar on Mössbauer Spectroscopy (OSSM 24)

Study of the Influence of Multi-Walled Carbon Nanotubes Functionalised with Nickel Ions on the Functioning of Red Blood Cells

S. STRZELEC^a, A. SINIARSKI^{b,c}, J. KIECANA^{b,c}, G. GAJOS^{b,c},
J. KORECKI^d AND K. BURDA^{a,*}

^aAGH University of Krakow, Faculty of Physics and Applied Computer Science, al. Mickiewicza 30, 30-059 Kraków, Poland

^bJagiellonian University, Medical College, Pradnicka 80, 31-202 Kraków, Poland

^cThe John Paul II Hospital, Pradnicka 80, 31-202 Kraków, Poland

^dJerzy Haber Institute of Catalysis and Surface Chemistry, Polish Academy of Sciences, 30-239 Kraków, Poland

Doi: [10.12693/APhysPolA.147.31](https://doi.org/10.12693/APhysPolA.147.31)

*e-mail: kvetoslava.burda@fis.agh.edu.pl

Functionalised carbon nanotubes are a group of nanomaterials with many potential applications in bionanomedicine. However, they can also be toxic, especially those functionalised with metal ions. Carbon nanotubes enter cells easily. The research focused on investigating the acute effects of multi-walled carbon nanotubes with attached Ni²⁺ ions (MWCNTs-Ni) on the functioning of red blood cells. The very low concentration of MWCNTs-Ni used did not cause changes in the size and shape of red blood cells, but it did affect the states of haemoglobin and its ability to reversibly bind oxygen. MWCNTs-Ni-treated red blood cells showed an increased affinity for O₂, similar to that observed in red blood cells from essential hypertensive subjects. The results indicate a potential risk that MWCNTs-Ni may influence the development of hypertension.

topics: multi-walled carbon nanotubes, erythrocytes, Mössbauer spectroscopy, haemoglobin

1. Introduction

Functionalised carbon nanotubes (CNTs) are promising nanomaterials for applications in many fields, especially in biophysics and nanomedicine. This is due to their unique physicochemical properties and biocompatibility [1]. Nanotechnology is playing an increasingly important role in medicine, for example through the use of nanoparticles that allow for higher-resolution imaging of cells, tissues, and whole organisms, and nanostructures that act as nanocarriers in targeted therapies. CNTs are the subject of intense research due to their relatively easy functionalisation, which is very important for the control of their interactions with biological systems [2, 3]. Another promising application of CNTs is their use in the production of implants. They can be used, for example, in dentistry [4] or in retinal regeneration [5].

The issue of toxicity and biodistribution of CNTs is still controversial [6]. Research is needed to clarify these issues [7, 8]. Carbon nanotubes can trigger toxic effects at both cellular and organismal levels [9]. At the cellular level, they can induce oxidative stress, DNA damage, apoptosis,

inflammation, and changes in the cellular cytoskeleton. They can cause inflammatory reactions in the body, damage lung tissue, and affect the functioning of the immune system. In order to better understand the mechanisms of toxicity of CNTs and their impact on human health, it is necessary to consider the potential routes of entry into the body, such as inhalation, ingestion (e.g., through food contamination), and absorption through the skin. In addition, toxicity testing of CNTs should take into account the differences between their structure and functional groups, as these may significantly affect the biological reactivity of these carbon nanomaterials. It has been shown that long-term exposure to CNTs can lead to the development of cancer [10, 11]. Intravenous administration of single-walled carbon nanotubes (SWCNTs) to mice resulted in transient anaemia. Older red blood cells were preferentially lysed [10]. Incubation of erythrocytes *in vitro* in the presence of acid SWCNTs induces lysis. This is dose- and time-dependent. Damage to the membrane is indicated by the formation of hydrophobic patches on the surface of the cells and by the externalisation of phosphatidylserine [12]. In addition, bundled SWCNTs were found to be more toxic than single SWCNTs, causing significant changes in the

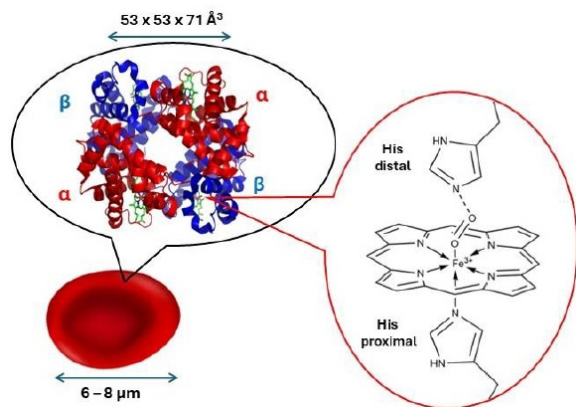


Fig. 1. Diagram showing the shape and average diameter of an erythrocyte, the structure of type A haemoglobin (HbA — the most abundant in adult human blood), consisting of two α globins and two β globins, each containing a haem group. On the right-hand side, the bond between the O_2 molecule and the haem iron (hexa-coordinate) is shown for oxyhaemoglobin (oxyHb). The scheme is based on [22–25].

shape and fusion of erythrocytes [13]. Functionalised CNTs can be designed to increase their biocompatibility and targeting capabilities. This further enhances their effectiveness as drug delivery vehicles. Functionalisation increases the ability of CNTs to penetrate into cells, which can be achieved by a variety of mechanisms, including endocytosis and passive diffusion [14–17]. Therefore, further research on the toxicity of carbon nanotubes is necessary to assess their safety and develop appropriate regulatory strategies aimed at minimising potential risks to health and the environment [18–21].

Our research presented here is specifically focused on the investigation of the potential risk of exposure of living organisms to metal-functionalised CNTs. The effects of CNTs on the cardiovascular system and the associated risk of developing civilisation diseases such as hypertension are of particular interest to us. Nanoparticles can easily enter the bloodstream. Red blood cells (RBCs) are therefore most exposed to their effects.

This paper presents *in vitro* studies of the acute effect of micromolar concentrations of multi-wall carbon nanotubes (MWCNTs) with attached nickel ions on healthy human red blood cell function (Fig. 1, see also [22–25]). MWCNTs are often more toxic than SWCNTs due to their larger surface area and are increasingly being used in nano(bio)technologies [26]. Long-term (several hours) effects of higher doses of carbon nanotubes on erythrocytes can be found in the literature [13]. However, it cannot be ruled out that low concentrations of CNTs, which do not cause rheological changes in RBCs, may already affect their function of supplying O_2 to the cells.

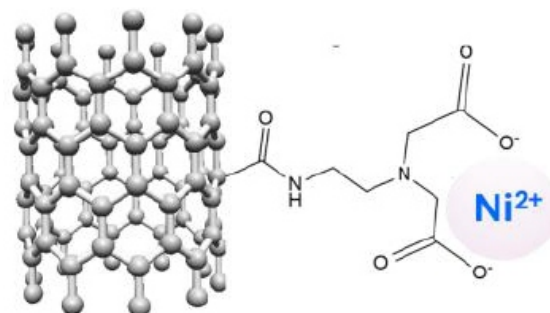


Fig. 2. Visualization of the method of connecting the nickel cation to a carbon nanotube using an IDA (iminodiacetic acid)-type complexation.

Mössbauer spectroscopy applied in this research is a unique technique that allows the study of all states of iron (including diamagnetic states) and thus, different types of haemoglobin, physiological and non-physiological [27–30]. The hyperfine parameters are sensitive to both the valence and spin states of haem iron (HFe) and to the nature and organisation of its ligands (binding site symmetry) [28, 31–34]. It is also possible to measure the oxygen saturation of Hb over time, which has been used to test the ability of the haemoglobin contained in red blood cells to bind O_2 in a reversible manner [35].

The aim of this research is to understand the effect of multi-walled carbon nanotubes with attached Ni^{2+} ions (MWCNTs-Ni) on RBC functioning and to highlight the potential risks to cells from even short-term exposure to metal-functionalised carbon nanotubes.

2. Materials and methods

2.1. Sample preparation

Blood samples were obtained from a healthy middle-aged female donor at the John Paul II Hospital in Kraków (Poland). Sodium heparinate was used to anticoagulate the blood drawn. All experiments were approved by the local Bioethics Committee of Physicians (317/KBL/OIL/2019).

Isolation and purification of red blood cells (RBC) were carried out according to the procedure previously described in [35, 36]. Finally, the sample contained isolated RBCs of a concentration of 1.65×10^9 cells/ml. The cells were suspended in phosphate buffer (5 mM NaH_2PO_4/Na_2HPO_4 , 0.15 M NaCl, pH 7.4) and divided into two fractions. The first fraction, designated RBC_{control}, was not further treated with functionalised carbon nanotubes and served as the control sample. The second fraction, designated RBC_{MWCNT_Ni 1:1000}, was

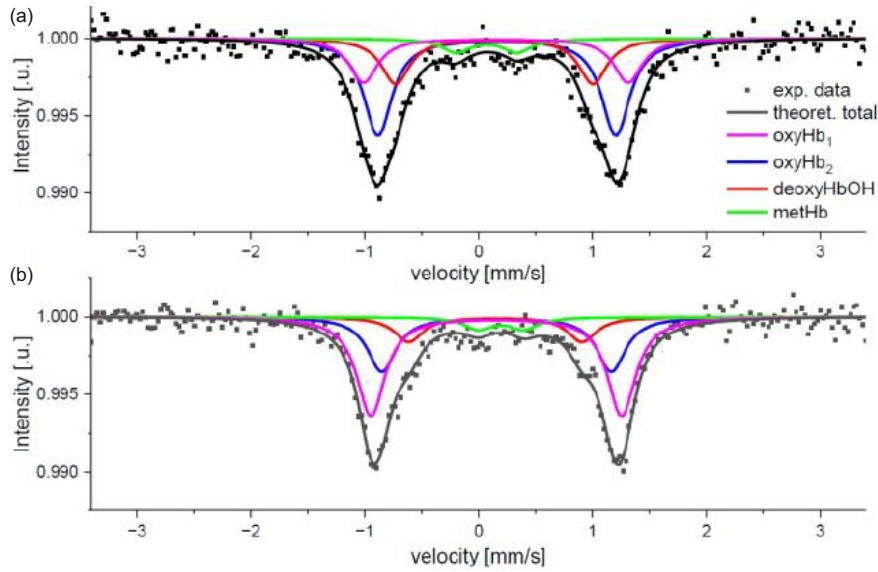


Fig. 3. Example Mössbauer spectra of $\text{RBC}_{\text{control}}$ measured after 5 h (a) and of $\text{RBC}_{\text{MWCNT_Ni 1:1000}}$ measured after 6 h (b). The symbols and lines are explained in the figure legend.

treated with functionalised multi-walled carbon nanotubes. Both fractions had a volume of 5 ml. The samples were incubated for 10 min at room temperature under dark conditions with constant mixing. Subsequently, they were washed a total of three times in phosphate buffer solution and then centrifuged. The resulting sediment was collected and stored at a temperature of -80°C until further analysis.

The material used was multi-walled carbon nanotubes (MWCNTs) with an average diameter of ≈ 20 nm [37, 38]. During the functionalisation process, nickel (II) ions were attached to the nanotubes (as shown in Fig. 2). The initial sample, comprising a suspension of MWCNTs-Ni in distilled water, was subjected to sonication for a period of 2 min prior to its addition to the RBCs. The final concentration of nanotubes in the sample $\text{RBC}_{\text{MWCNT_Ni 1:1000}}$ was $5.9 \mu\text{g/ml}$.

Both samples were analysed in an optical microscopy (Olympus IX71, Japan) to determine their dimensions and shapes. This was achieved by examining 100 randomly selected control RBCs and those treated with MWCNTs-Ni.

2.2. Mössbauer spectroscopy measurements

The types of haemoglobin present in RBCs and the reversible oxygen attachment to haemoglobin (Fig. 1) were investigated using Mössbauer spectroscopy, as described in [35]. The measurements utilised a home-made cryostat that allowed for gas exchange, with a 100-mCi ^{57}Co (Rh) source providing the radiation with an energy of 14.4 keV. The measurements were carried out at a temperature

of $85 \pm 0.1^{\circ}\text{C}$, and spectra were recorded every 30 min for up to 24 h. The analysis of the collected spectra was performed using Recoil software [39].

3. Results and discussion

The mean diameter of the control RBCs was found to be $6.38 \pm 0.21 \mu\text{m}$, and that of the sample incubated in the presence of nanotubes was $6.17 \pm 0.21 \mu\text{m}$. Information about the shape of the erythrocytes was provided by the determined ovality of the RBCs based on the ratio of the longitudinal diameter to the transverse diameter. For the $\text{RBC}_{\text{control}}$ and $\text{RBC}_{\text{MWCNT_Ni 1:1000}}$, it was 1.045 ± 0.045 and 1.046 ± 0.056 , respectively. The results show that MWCNTs-Ni at the concentration used did not alter the shape of the erythrocytes. However, a slight reduction in cell size of $\approx 0.2 \mu\text{m}$ was observed on average. Nevertheless, this reduction is within the error range.

However, the results of Mössbauer spectroscopy indicate that the functionality of RBCs treated with the carbon nanotubes differs significantly from that of the control sample (Figs. 3–5). In both cases, spectra collected after a longer period required the consideration of at least four components. This is demonstrated by the example spectra obtained for $\text{RBC}_{\text{control}}$ and $\text{RBC}_{\text{MWCNT_Ni 1:1000}}$ presented in Fig. 3a and b, respectively.

In the case of RBCs treated with MWCNTs-Ni, two components, due to their characteristic hyperfine parameters and time evolution, are assigned to oxyHbs. The component whose hyperfine parameters are $\text{IS} = 0.16 \pm 0.01 \text{ mm/s}$

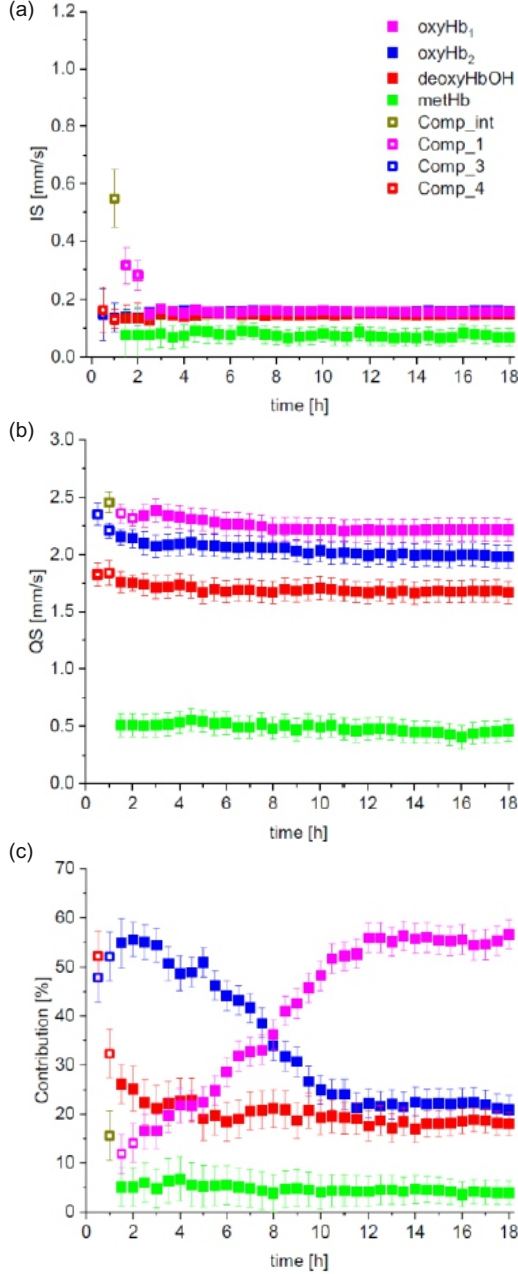


Fig. 4. The time evolution of the (a) isomeric shift, (b) quadrupole splitting, and (c) contribution of different haemoglobin components in $RBC_{control}$. The symbols are explained in the figure legend.

and $QS = 2.20 \pm 0.04$ mm/s is called $oxyHb_1$. The second one with $IS = 0.17 \pm 0.01$ mm/s and $QS = 1.95 \pm 0.06$ mm/s is called $oxyHb_2$. Both have their own precursors, which appear in the spectra for the initial measurement times up to ≈ 2.5 h after treating the sample with high N_2 pressure and removing O_2 . The temporal evolution of the hyperfine parameters (IS — isomeric shift and QS — quadruple split) of the individual haemoglobin forms and their fractions are shown in Fig. 5a–c. As can be seen in Fig. 5c, Comp_1 passed partly directly and

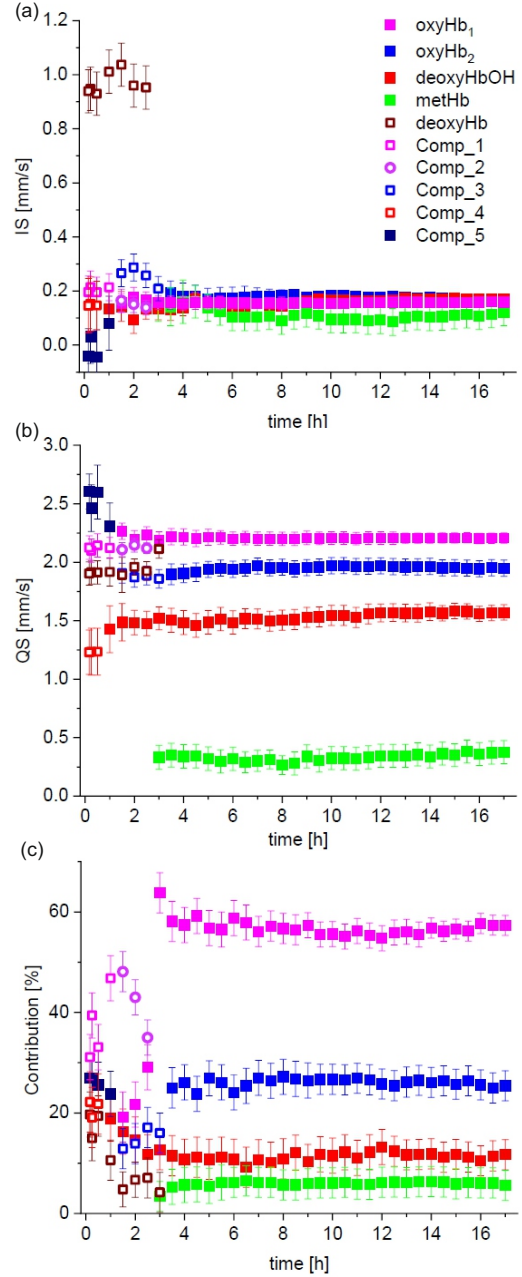


Fig. 5. The time evolution of the (a) isomeric shift, (b) quadrupole splitting, and (c) contribution of different haemoglobin components in $RBC_{MWCNT_Ni\ 1:1000}$. The symbols are explained in the figure legend.

partly indirectly through Comp_2 into $oxyHb_1$. In turn, Comp_3 evolved towards $oxyHb_2$. Comp_4 ultimately converted to $deoxyHbOH$ with $IS = 0.17 \pm 0.01$ mm/s and $QS = 1.6 \pm 0.06$ mm/s (red component in Fig. 3b). Figure 3b also shows methHb with a small isomeric shift and quadrupole splitting ($IS = 0.10 \pm 0.05$ mm/s and $QS = 0.40 \pm 0.10$ mm/s). MethHb evolved from $deoxyHbOH$, as indicated by the conserved sum of their contributions to the spectra for times > 2.5 h (Fig. 5c). During the initial

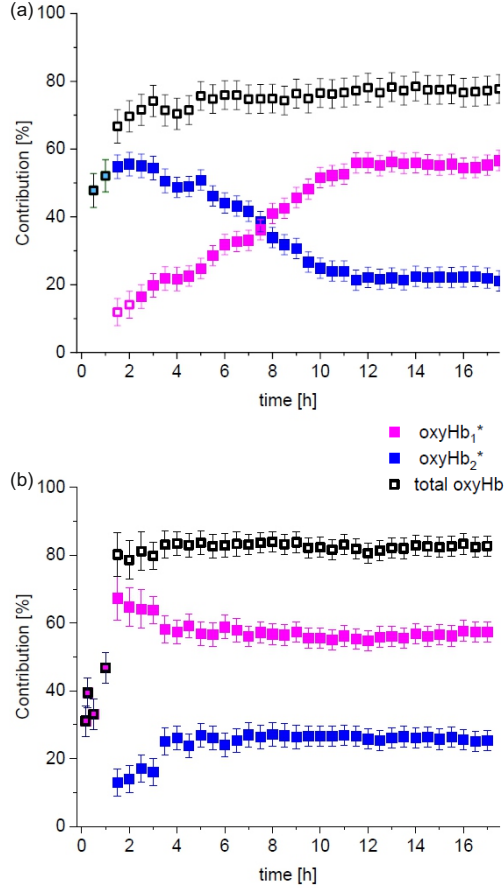


Fig. 6. Time evolution of the contributions of different forms of oxyhaemoglobin in (a) untreated RBCs and (b) treated with MWCNTs-Ni. The designations oxyHb_1^* and oxyHb_2^* mean that all forms of oxyhaemoglobin that were precursors of oxyHb_1 and oxyHb_2 , respectively, were included for the initial times (see main text and Figs. 4c and 5c).

three-hour period, deoxyHbOH also partially transformed into oxyHb_2 . During the same period of time, deoxyHb was in saturation with oxygen and was converted to oxyHb_1 . Comp_5, with an isomeric shift near 0 mm/s and a quadrupole splitting of about 2.5 mm/s, indicating a significant nitrogen effect on this haemoglobin form, converted to Comp_1, the precursor of oxyHb_1 .

In the control sample (Figs. 3 and 4), both oxyHb_1 and oxyHb_2 exhibited similar hyperfine parameters, in line with the observations made for RBCs treated with carbon nanotubes. However, the higher quadrupole splitting of oxyHb_2 ($QS = 2.05 \pm 0.09$ mm/s) was notable (Fig. 4b). The average IS values of oxyHbOH and metHb were found to be lower by approximately 0.02 and 0.04 mm/s, respectively (Fig. 4a), while their quadrupole splittings were higher by ≈ 0.1 mm/s in both cases for $\text{RBC}_{\text{control}}$ (Fig. 4b). An intermediate state of deoxyHb (called Comp_int, see Fig. 4) was detected in untreated RBCs, but quickly converted

to oxyHb_1 via Comp_1. Comp_3, which converted to oxyHb_2 , had a lower IS but a higher QS than in the MWCNTs-Ni treated RBCs (Fig. 4a and b). In the initial four hours of the control sample, deoxyHbOH underwent partial conversion to oxyHb_1 and oxyHb_2 , with a final concentration of $\approx 20\%$. The precursor of deoxyHbOH, i.e., Comp_4, was characterised by higher IS and QS values than for $\text{RBC}_{\text{MWCNT-Ni 1:1000}}$. Over time, its contribution to the spectra decreased slightly, resulting in a gradual increase in total oxyHb contribution, as visible in Figs. 4c and 6a.

Nonetheless, the most pronounced contrasts between $\text{RBC}_{\text{control}}$ and $\text{RBC}_{\text{MWCNT-Ni 1:1000}}$ that were observed in Mössbauer experiments were a consequence of the temporal evolution of distinct forms of oxyhaemoglobin (Figs. 4c and 5c). Figure 6 provides further illustration of the changes in total oxyHb over time for each system. Firstly, the control sample for times < 8 h was dominated by oxyHb_1 , the proportion of which decreased over time from around 55% to around 22%. This was accompanied by a gradual increase in the fraction of oxyHb_2 , which stabilised at around 57%. In contrast, for the MWCNTs-Ni treated sample, the oxyHb_2 component dominated over the whole time range. Its contribution for times > 1.5 h gradually decreased to stabilise at a level of about 57%, i.e., similar to that of the control sample. OxyHb_1 reached a slightly higher level compared to the control sample, and therefore the final saturation in $\text{RBC}_{\text{MWCNT-Ni 1:1000}}$ was about 3% higher than in $\text{RBC}_{\text{control}}$. Moreover, the increase in the oxyhaemoglobin fraction in the initial period was steeper in the RBCs treated with carbon nanotubes than in the untreated RBCs.

4. Conclusions

The low concentration of Ni^{2+} ion functionalised MWCNTs (5.9 $\mu\text{g}/\text{ml}$) did not result in significant changes in the size and shape of the erythrocytes compared to the control sample. The results obtained using Mössbauer spectroscopy showed the presence of different forms of haemoglobin characterised by hyperfine parameters. These parameters indicate different conformations of the O_2 binding site within the Hb globin pocket. They may result from both the symmetry of the HF-Fe-O_2 bond itself (e.g., length and angle of the bond, position of the Fe ion relative to the heme porphyrin plane) and the binding of heme to globins, in particular their rigidity. However, studies on the reverse binding of oxygen to haemoglobin showed a significant difference between the control RBCs and those treated with MWCNTs-Ni. In the latter case, on the one hand, oxygen was released much more easily under the low partial pressure of oxygen, and on the other hand, it was incorporated much more effectively when the

partial pressure of oxygen increased. This behaviour is very reminiscent of a phenomenon that has previously been observed in the erythrocytes of people suffering from primary arterial hypertension [35]. This could be an indication of a potential risk of the impact of metal-functionalised carbon nanotubes on the development of high blood pressure when they are present in the blood circulation, even at very low concentrations. Further research is currently being carried out in this direction.

Acknowledgments

The work was supported by the National Science Centre, Poland, grant no. 2019/33/B/NZ7/02724.

References

- [1] B.O. Murjani, P.S. Kadu, M. Bansod, S.S. Vaidya, M.D. Yadav, *Carbon Lett.* **32**, 1207 (2022).
- [2] M. Saeedimasine, E.G. Brandt, A.P. Lyubartsev, *J. Phys. Chem. B* **125**, 416 (2021).
- [3] X. Han, S. Li, Z. Peng, A.O. Al-Yuobi, A.S. Omar Bashammakh, M.S. El-Shahawi, R.M. Leblanc, *J. Oleo Sci.* **65**, 1 (2016).
- [4] S.J. Teh, C.W. Lai, *Carbon Nanotubes for Dental Implants, Applications of Nanocomposite Materials in Dentistry*, 2019, p. 93.
- [5] C.G. Eleftheriou, J.B. Zimmermann, H.D. Kjeldsen, M. David-Pur, Y. Hanein, E. Sernagor, *Biomaterials* **112**, 108 (2017).
- [6] J.T. Wang, N. Rubio, H. Kafa et al., *J. Control Release* **224**, 22 (2016).
- [7] Y. Liu, Y. Zhao, B. Sun, C. Chen, *Acc. Chem. Res.* **46**, 702 (2013).
- [8] M.A. Saleemi, M. Hosseini Fouladi, P.V.C. Yong, K. Chinna, N.K. Palanisamy, E.H. Wong, *Chem. Res. Toxicol.* **34**, 24 (2021).
- [9] K. Pulskamp, S. Diabaté, H.F. Krug, *Toxicol. Lett.* **168**, 58 (2007).
- [10] K. Kostarelos, *Nat. Biotechnol.* **26**, 774 (2008).
- [11] C.A. Poland, R. Duffin, I. Kinloch, A. Maynard, W.A. Wallace, A. Seaton, V. Stone, S. Brown, W. Macnee, K. Donaldson, *Nat. Nanotechnol.* **3**, 423 (2008).
- [12] S. Sachar, R.K. Saxena, *PLoS One* **6**, e22032 (2011).
- [13] Y. Heo, C.A. Li, D. Kim, S. Shin, *Clin. Hemorheol. Microcirc.* **65**, 49 (2017).
- [14] A. Bianco, K. Kostarelos, M. Prato, *Curr. Opin. Chem. Biol.* **9**, 674 (2005).
- [15] N.W.S. Kam, M. O'Connell, J.A. Wisdom, H. Dai, *Proc. Natl. Acad. Sci.* **102**, 11600 (2005).
- [16] X. Zhang, L. Meng, Q. Lu, Z. Fei, P.J. Dyson, *Biomaterials* **30**, 6041 (2009).
- [17] N.W.S. Kam, H. Dai, *J. Am. Chem. Soc.* **127**, 6021 (2005).
- [18] A. Schinwald, F.A. Murphy, A. Jones, W. MacNee, K. Donaldson, *ACS Nano* **6**, 736 (2012).
- [19] K. Donaldson, F.A. Murphy, R. Duffin, C.A. Poland, *Part. Fibre Toxicol.* **7**, 5 (2010).
- [20] K. Donaldson, C.A. Poland, F.A. Murphy, M. MacFarlane, T. Chernova, A. Schinwald, *Adv. Drug Deliv. Rev.* **65**, 2078 (2013).
- [21] H. Dumortier, S. Lacotte, G. Pastorin, R. Marega, W. Wu, D. Bonifazi, J.P. Briand, M. Prato, S. Muller, A. Bianco, *Nano Lett.* **6**, 1522 (2006).
- [22] G. Brecher, E.F. Jakobek, M.A. Schneiderman, G.Z. Williams, P.J. Schmidt, *Ann. NY Acad. Sci.* **99**, 242 (1962).
- [23] W.L. Bragg, E.R. Howells, M.F. Perutz, *Proc. R. Soc. A* **222**, 33 (1997).
- [24] P.J. Derry, A.T.T. Vo, A. Gnanasekaran, J. Mitra, A.V. Liopo, M.L. Hegde, A.L. Tsai, J.M. Tour, T.A. Kent, *Front. Cell Neurosci.* **14**, 603043 (2020).
- [25] L.W. Wilkins, *Clinical Hematology: Theory and Procedures*, 2004.
- [26] J. Simon, E. Flahaut, M. Golzio, *Materials (Basel)* **12**, 624 (2019).
- [27] G. Lang, W. Marshall, *Proc. Phys. Soc.* **87**, 3 (1966).
- [28] E.R. Bauminger, I. Nowik, *Hyperfine Interact.* **111**, 159 (1998).
- [29] M. Cyrklaff, S. Srismith, B. Nyboer et al., *Nat. Commun.* **7**, 13401 (2016).
- [30] J. Fiedor, M. Przetocki, A. Siniarski, G. Gajos, N. Spiridis, K. Freindl, K. Burda, *Acta Phys. Pol. A* **139**, 283 (2021).
- [31] E. Bradford, W. Marshall, *Proc. Phys. Soc.* **87**, 731 (1966).
- [32] K. Burda, A. Hryniewicz, H. Kołoczek, J. Stanek, K. Strzałka, *Biochim. Biophys. Acta* **1244**, 345 (1995).
- [33] J. Fiedor, M. Przetocki, A. Siniarski, G. Gajos, N. Spiridis, K. Freindl, K. Burda, *Antioxidants (Basel)* **10**, 451 (2021).

- [34] M. Kaczmarska, Z. Kopyściańska, M. Fornal, T. Grodzicki, K. Matlak, J. Korecki, K. Burda, *Acta Biochim. Pol.* **58**, 489 (2011).
- [35] M. Kaczmarska, M. Fornal, F.H. Messerli, J. Korecki, T. Grodzicki, K. Burda, *Cell Biochem. Biophys.* **67**, 1089 (2013).
- [36] K. Niemiec, M. Kaczmarska, M. Buczkowski, M. Fornal, W. Pohorecki, K. Matlak, J. Korecki, T. Grodzicki, K. Burda, *Hyperfine Interact.* **206**, 95 (2011).
- [37] K. Luberda-Durnaś, M. Nieznalska, M. Mazurkiewicz et al., *Phys. Status Solidi (a)* **208**, 1796 (2011).
- [38] A. Jamrozik, M. Mazurkiewicz, A. Małolepszy, L. Stobiński, K. Matlak, J. Korecki, K.J. Kurzydłowski, K. Burda, *Phys. Status Solidi (a)* **208**, 1783 (2011).
- [39] D.G. Rancourt, J.Y. Ping, *Nucl. Instrum. Methods Phys. Res. B* **58**, 85 (1991).